

Temperature Dependent Etching of (100) and (110) Silicon in NaOH and in Tetramethyl-Ammonium Hydroxide

Vladimir F. Kleptsyn and Johannes G. Smits

Department of Electrical and Computer Engineering
College of Engineering, Boston University
8 Saint Mary's Street, Boston MA 02215, U.S.A.

(Received February 2, 2002; accepted December 4, 2002)

Key words: silicon, wet etching, sodium hydroxide, tetramethyl ammonium hydroxide

The etch rates for single crystal silicon wafers in NaOH and tetramethyl-ammonium hydroxide (TMAH) have been measured in the temperature range from 28°C to 80°C and activation energies of about 0.68 and 0.57 eV for NaOH and TMAH respectively for the (100) plane are observed. A qualitative model of the etching of silicon planes in NaOH and TMAH is presented.

1. Introduction

Orientation dependent etching of silicon has been studied in the past using aqueous solutions of alkali hydroxides. It is a very useful technique to fabricate microstructures in silicon. Weirauch⁽¹⁾ studied anisotropic etching of single crystal silicon spheres and wafers using 10 M KOH as the etchant. The etch rates along several vector directions were measured and the slowest etching planes were found using a single crystal sphere. Using these data, a method was developed to predict the angles of inclination for surfaces of different orientations. The angles of inclination correlated well with the data collected from etching a single crystal sphere. Kendall *et al.*⁽²⁾ proposed the new wagon wheel method to measure anisotropic etching. So far several studies have been carried out to understand the mechanism of etching and, based on the experimental data obtained, several models for etching have been proposed. Glembocki *et al.*⁽³⁾ measured etch rates for the

(100) and (110) surfaces in KOH using the wagon wheel method and proposed that the large dependence of etch rates on crystal orientation may be due to geometry and the way hydration complexes interact with various crystal surfaces. Seidel⁽⁴⁾ studied the etch rates of (100) silicon and silicon dioxide in KOH with respect to temperature and crystal orientation with respect to the (111) plane. The etch rates of (100) silicon and silicon dioxide were found to increase with increasing temperature and to reach a limit with a further increase in the concentration, after which a decrease of the etch rate with concentration was observed. Based on the results, they proposed a mechanism of etching. De Guel *et al.*⁽⁵⁾ measured lateral etch rates for four different concentrations of KOH over a range of temperatures for 45 different crystal orientations around the (100) pole and obtained heart shaped curves with a minimum etch rate in the [100] direction. Seidel *et al.*⁽⁶⁾ studied anisotropic etching of single crystal silicon and also the behavior of SiO₂ and Si₃N₄ in KOH at different temperatures and concentrations of the etchant. The various crystal planes bounding the etch front and their etch rates were determined as a function of temperature, crystal orientation and etchant composition; they proposed an electrochemical model for etching of silicon. Seidel and coworkers found that various concentrations of KOH and different temperatures did not have any effect on Si₃N₄. Allongue *et al.*⁽⁷⁾ observed a combination of electrochemical and chemical processes controlling the etching of silicon in NaOH solutions and recorded the orientation dependence of the electrochemical processes. A detailed reaction mechanism including splitting Si-H and Si-Si bonds as the part of the etching process was also presented in this paper. Sato *et al.*⁽⁸⁾ measured etch rates in various vector directions using a hemispherical concave specimen in a 40% KOH aqueous solution for different temperatures. Using these results Koide *et al.*⁽⁹⁾ and Sequin⁽¹⁰⁾ developed a simulation program for the two-dimensional etching profile designing fabrication processes of the micro mechanical silicon devices. Later a few more simulations programs, MICROCAD and SIMODE, were developed by Sato with coworkers⁽¹¹⁾ and Fruehauf with co-authors.⁽¹²⁾ Recently van Veenendaal and co-authors presented a simulation of wet chemical etching using a physical model⁽¹³⁾ and Horn *et al.* developed a step flow model for orientation-dependent etching of silicon.⁽¹⁴⁾

Palik *et al.*⁽¹⁵⁾ suggested that orientation dependent etching could be due to mono layers of silicates or SiO₂ coating each atomic plane differently causing a difference in etching rates. Palik *et al.*⁽¹⁶⁾ measured the etching products by recording Raman spectra as the etching of (100) silicon progresses in 5 M aqueous KOH and found primary etching species to be OH⁻ and the etching products were determined to be SiO₂(OH)₂²⁻. Glembocki *et al.*⁽¹⁷⁾ proposed a mechanism to account for the orientation dependence of etch rates based on the difference in reactivity to nucleophilic attack of a silicon sample which is dependent on the number of dangling bonds in each plane. Palik *et al.*⁽¹⁸⁾ suggested that etching of silicon occurs by the attack of back bonds (bulk bonds) by H₂O and OH⁻ and concluded that orientation dependence must be caused by the shadowing of the bulk bonds and the ease or difficulty with which H₂O and OH⁻ react with bulk Si-Si bonds. Landsberger and coworkers in a series of papers⁽¹⁹⁻²¹⁾ investigated the anisotropic etching of silicon in TMAH at different temperatures and concentrations. Etch anisotropy is found to be different in 25wt% and 15wt% TMAH: shallow local minima at {110} planes were observed in the last case whereas in 25wt% TMAH there is a deep minimum at {100}.

Anisotropic etching of silicon in TMAH solutions has also been investigated in a series of papers⁽²²⁻²⁴⁾; the most detailed investigation was performed by M. Shikida with coworkers⁽²³⁾; silicon etch rates for both KOH and TMAH at various temperatures for various crystallographic planes have been measured and corresponding activation energies were estimated.

For simple structures such as inverted pyramids, the differences between various alkaline etchants are in their different etch rates of (100) and (111) planes. For many applications limited knowledge of the above two variables is sufficient to construct good products. However, for more complicated constructions, such as vertical walls or protruding pyramids, these two variables have to be augmented with etching rates and their temperature dependence of other planes and more profound understanding of the etching mechanisms of various planes in various etchants.

In our preliminary experiments we saw a significant difference in silicon etching in NaOH and in TMAH. The most interesting phenomenon was the difference in (100)/(111) etch rate ratios for those etchants: a few hundred for NaOH and about 30 for TMAH. In the present work we have tried to find the cause of this phenomenon; in order to understand that we have investigated the (100) and (110) silicon anisotropic etching in NaOH and TMAH at tightly controlled conditions. We have taken into consideration a geometrical factor (size of an ion) which allowed us to construct a microscopic model of etching processes on (100), (110) and (111) planes and to supplement Seidel's⁽⁶⁾ existing electrochemical microscopic models of silicon etching in alkaline solutions.

2. Experimental Methods

A few *n*-type (100) and (110) silicon wafers were cleaned, thermally oxidized (0.3 μm SiO_2 thickness), and the wagon wheel pattern with rectangular openings every 5° was transferred onto the wafers. These wafers were then etched for 12 minutes in buffered oxide etch (BOE) and rinsed in DI water. The photoresist was then removed. All the wafers were dipped in BOE for about 10 seconds just before beginning the etching process in NaOH or TMAH to remove any native oxide that was formed in the open slots.

Etching was performed in 50% NaOH aqueous solution and 25% TMAH aqueous solution. The beakers containing etchants were placed on standard laboratory hot plates, and the temperature was controlled manually to within 1°C of the required temperature. Etching was started when the temperature became stable.

After etching was completed, the etch rates of silicon were measured. The depth from the top to bottom of the slots was measured, averaged for several slots, and the etch rates of (100) and (110) planes in $\mu\text{m}/\text{h}$ were calculated. This procedure was applied for various temperatures. Also, the lateral underetched distances and averaged angle of underetching slopes were defined for all the slots on the (100) plane. The lateral underetched distances were measured by focusing on the top of the oxide overhang and measuring the distance of the edge of the underetched silicon. The average slope of the underetched surface was found by measuring the distance of the top to the floor of the underetched surface by focusing through the oxide.

3. Results and Discussion

The plots of etch rates vs. $1000/T$ (T : temperature in Kelvin) show the slopes to be constants when plotted using semilogarithmic graphs both for NaOH and TMAH (Fig. 1). We used the Arrhenius equation

$$r = r_0 e^{\frac{-E_a}{kT}}, \quad (1)$$

where r is the etch rate, E_a is the activation energy, r_0 is the pre-exponential factor, k is the Boltzmann constant, and T is the temperature in Kelvins. This equation was applied to the data and the plots so activation energies are found to be 0.68 eV for NaOH and 0.57 eV for TMAH for the (100) plane and corresponding pre-exponential factors to be $3.7 \times 10^{11} \mu\text{m}/\text{h}$ and $3.0 \times 10^9 \mu\text{m}/\text{h}$. The activation energies for the (110) plane are 0.61 eV and 0.42 eV for NaOH and TMAH correspondingly.

The difference of the activation energies for NaOH and TMAH as evident in Fig. 2 points to the different mechanisms of removal of atoms from surfaces while etching. A model to explain this difference is discussed later.

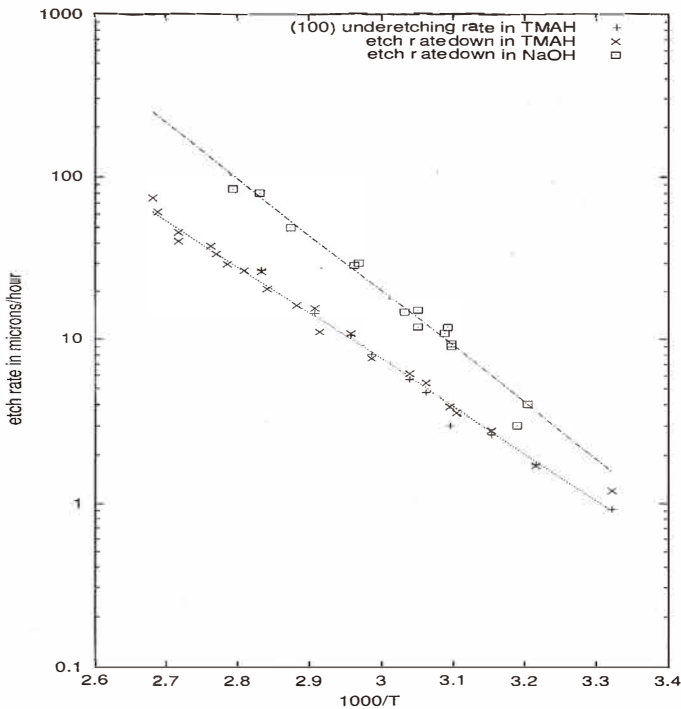


Fig. 1. Etch rates vs. inverse temperature for silicon (100) in TMAH and NaOH together with the best fitting lines. Corresponding activation energies and pre-exponential factors have been calculated.

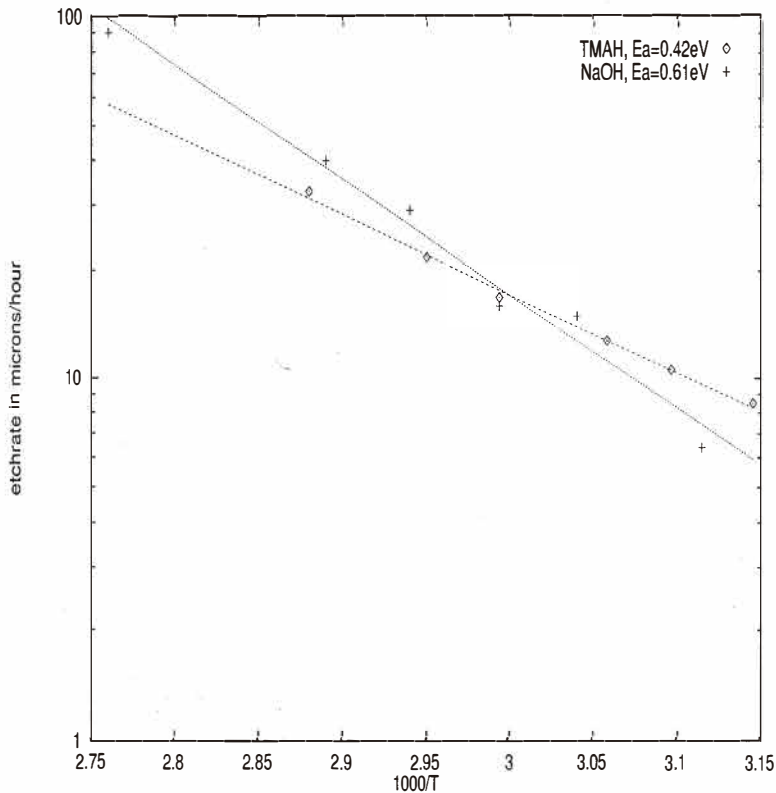


Fig. 2. Etch rates vs. inverse temperature for the silicon (110) plane in NaOH and TMAH.

In our measurements the etch rate of the {111} planes in TMAH is estimated to be about $1 \mu\text{m/h}$ at 90°C and about $0.25 \mu\text{m/h}$ at 40°C . So far, as it has been very difficult to measure the etch rate with sufficient accuracy, the activation energy may not be defined precisely as well. Our estimation gives $E_a = 0.2\text{--}0.4 \text{ eV}$. This is very close to $E_{a(111)} = 0.4 \text{ eV}$ given in ref. (22); in both cases the accuracy is very low but we can definitely say that in our experiments this value was much less than E_a for (100) planes and it points again to the difference in the mechanisms of etching. At the same time M. Shikida *et al.*⁽²³⁾ report activation energy to be 0.69 eV , but their measurements were performed only at three various temperatures. We did not set a goal to measure the etch rate of the (111) planes in NaOH. We only estimated the etch rate to be very low, 10–100 times less than in TMAH in the same temperature range, and we think that mechanisms of etching of (111) planes differ between NaOH and TMAH as it is pointed out in ref. (23) as well.

The lateral underetch rates when plotted as a function of slot orientation in the form of a polar plot resulted in a symmetric rosette, where an absolute minimum of underetching occurred in the [110] direction, (the horizontal and vertical slots in Fig. 3), and local

minima at [100] (the slots under 45°) both for NaOH and TMAH (Fig. 3).

The maximum lateral etch rate in TMAH occurs at the 25° slot, approximately equivalent to the {31n}-planes (this is in accordance with maximum (311)/(100) etch rate ratio given in ref. (23), whereas wafers etched in NaOH had maximum underetching at the 30°, 35° and even 40° slot. The maximum angle of inclination was 90° for the (100) plane—45° slots have vertical walls—for both etchants but other corresponding slots, except the 0° slot, appear completely different. Because of symmetry we consider slots from 0° to 45° only.

In the case of etching silicon in TMAH, all slots have smooth inclined surfaces faceted by {111} and {311} planes (0°, 5°, 10°, 15° slots) or nonfaceted surfaces (20°, 25°, 30° and 40° slots). In case of NaOH, all slots (except the 0° slot) have rough surfaces faceted mostly by {111} planes. So far as {111} planes are almost not being etched in NaOH, these planes define the inclination angle that can be measured only as an “average” slope of a zigzag surface. These results confirm one more time that mechanisms of (100) and (111) silicon etching in NaOH and TMAH are different.

In case of etching of the (100) plane, the microscopic model and corresponding chemical reactions were presented by Seidel with co-authors.⁽⁶⁾ In this model the nature of

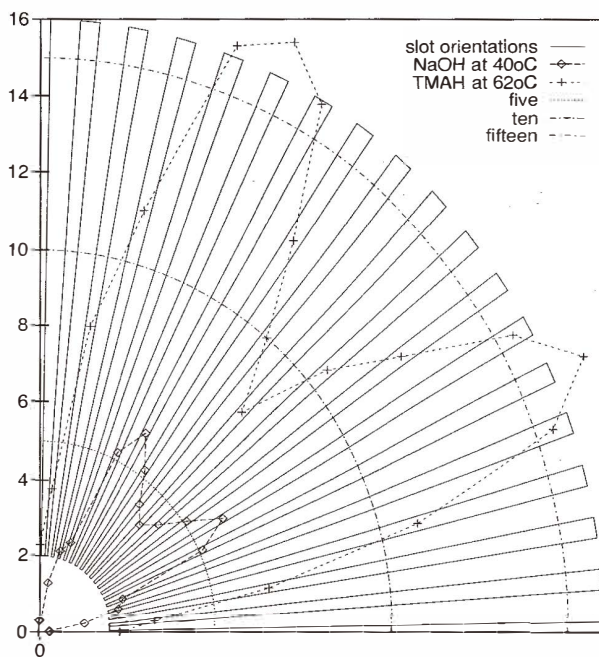


Fig. 3. Polar diagram for underetching rate ($\mu\text{m/h}$) in various directions for NaOH at 40°C (diamonds) and TMAH at 62°C (plus signs). The slot orientations are given here merely as visual aids. In the real mask, the slots were rectangles bordered by parallel lines, one slot every five degrees, while in this plot, the slots are drawn as radial slots with a width of two degrees centered around multiples of 5 degrees. The X- and Y-axes of the plot correspond to [110] crystallographic directions.

the cation has not been taken into consideration; so far as all measurements (including ours) of activation energies in various etchants^(6,22,23) are close, 0.6 eV in order of magnitude, we believe that the mechanism of etching is the same for all etchants.

A more complex situation takes place in case of the etching of {111} planes. In order to understand these processes in NaOH and TMAH, the following supplement to the microscopic model⁽⁶⁾ is presented. It may explain the etching process at least qualitatively. The positively charged ions or groups (Na^+ in NaOH, TMA^+ in TMAH) are being attracted to the silicon surface, because of its negative potential created by electrons coming from an electrolyte (electrochemical model of etching in ref. (6)); that attraction is also in agreement with Allongue's STM investigation of silicon surface covered by hydrogen⁽²⁵⁾ and interact with silicon due to its dangling bond(s). In this situation, the positively charged ion forms a dipole with the surface silicon atom which is negatively charged by the attracted electron. The dipole field is present around the dipole vectors. The OH^- groups, which are dipoles in their own right, can align themselves antiparallel with the existing dipole fields.

Four different situations for Na^+ on (100) and (111) planes and for TMA^+ on (100) and (111) surfaces are shown in Figs. 4(a) – 4(d). In case of Na^+ on the (100) plane, each atom of the Si-surface is bonded with Na^+ over it, as shown in Fig. 4(a) below:

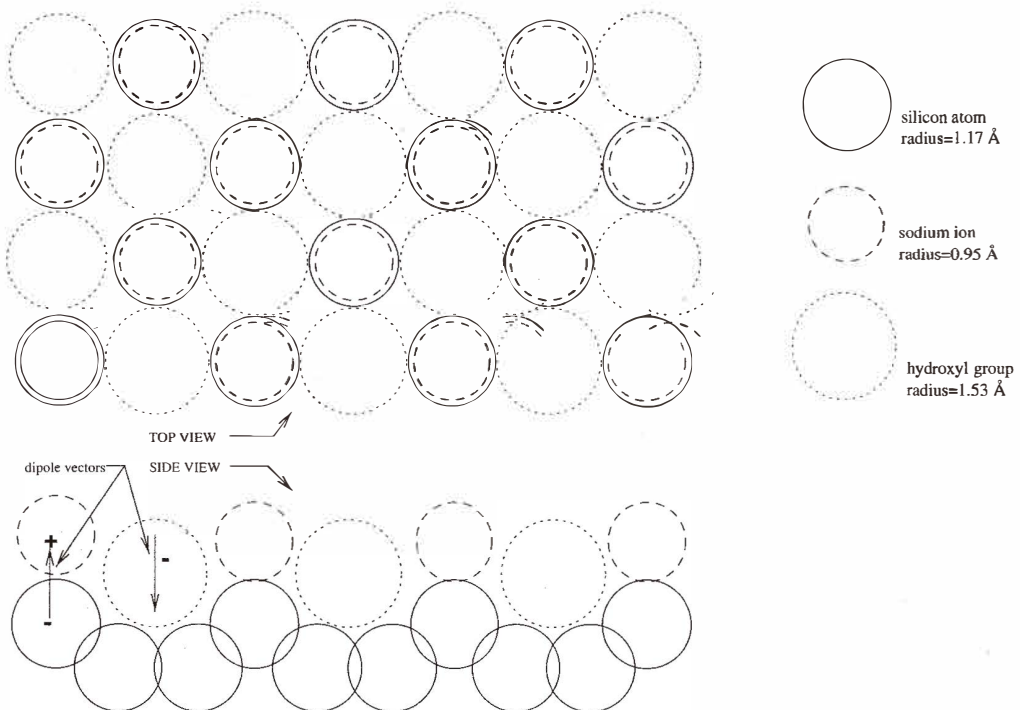


Fig. 4(a). In this figure, the location of the sodium ions is shown on top of the silicon (100)-plane atoms, along with the locations of the OH groups.

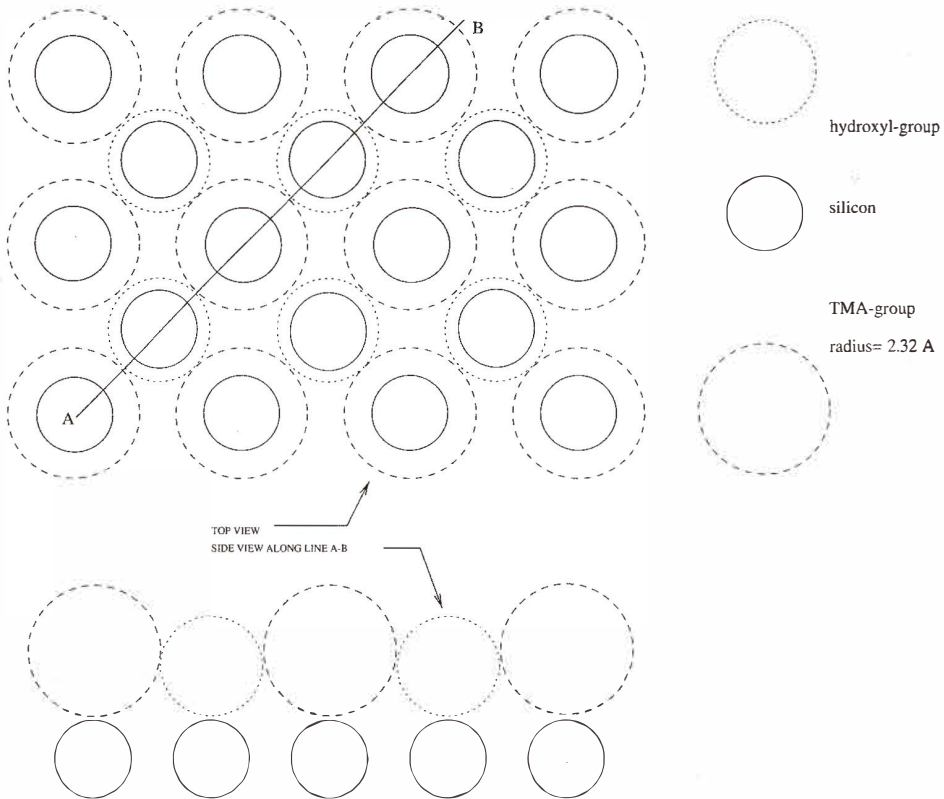


Fig. 4(b). In this figure, the location of the TMA⁺ groups is shown on top of the silicon atoms in the (100) plane, along with the locations of the OH groups.

While the TMA⁺ group has a larger size than the sodium atom, not all Si atoms in the surface can be bonded with a TMA⁺ because of volume constraints, so at most only one half of the number of the silicon atoms is covered by the TMA⁺ groups (Fig. 4(b)).

In both of these cases, there is sufficient space for the OH⁻ groups to penetrate through the layer of positively charged ions to the wafer and interact with silicon. We observe etching, we can measure the etching rate and the corresponding activation energy.

In the case of Na⁺ on the (111) plane (Fig. 4(c)), we can see that each atom of the Si-surface is also connected with Na⁺ but there is no more access for an OH⁻ group to the silicon surface: the maximum radius of an ion which could pass through is 1.27 Å, whereas $r_{\text{OH}^-} = 1.53 \text{ \AA}$. In fact, Na⁺ ions block the (111) silicon surface for OH⁻ groups so we have an extremely low etch rate.

Now consider the (111) silicon surface in TMAH (Fig. 4(d)).

Positively charged TMA⁺ groups may be bonded only with each fourth silicon atom just because of their size ($r = 2.32 \text{ \AA}$). In this case, the maximum radius of an ion that could pass

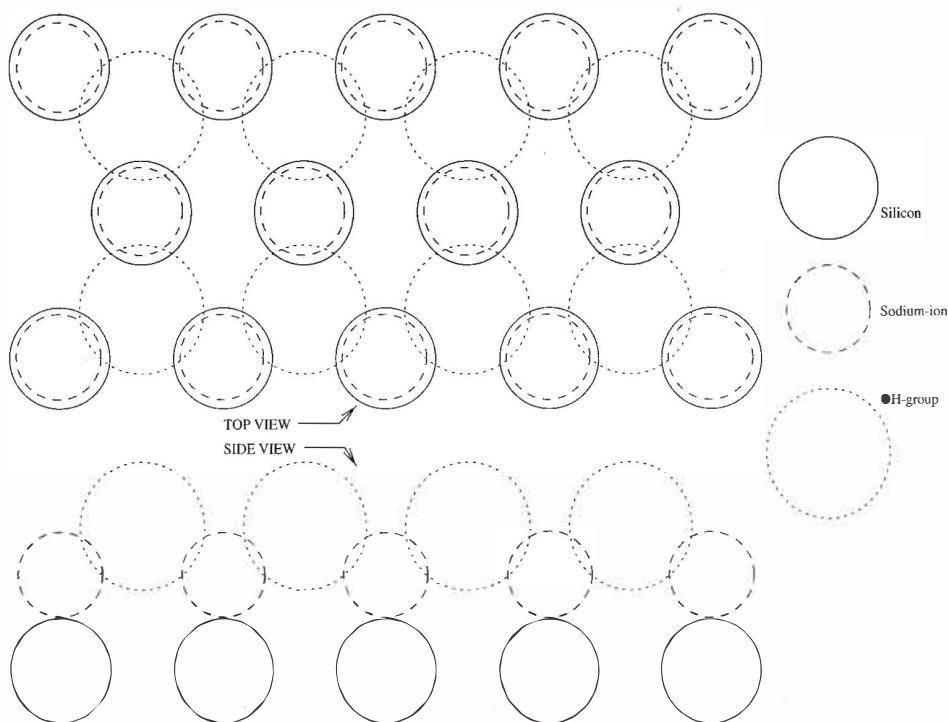


Fig. 4(c). In this figure, the location of the sodium ions is shown on top of the (111) plane silicon atoms, along with the locations of the OH groups.

through is 2.11 Å, so OH⁻ groups may have access to the silicon surface and attack binding (bulk) bonds. Each of the silicon surface atoms not underlying TMA⁺ groups may interact with two OH⁻ groups. We assume a TMA⁺ group plays a role of a catalyst gathering six OH⁻ groups with antiparallel dipole moments around itself and letting them attack binding bonds.

In all of those cases the OH⁻ groups play an important role of “removing agent,” making etch products soluble. That is in accordance with models presented by Seidel *et al.*⁽⁶⁾ and Allongue *et al.*⁽⁷⁾

Now let us go back to the consideration of the silicon (111) plane etching process. In order to remove one atom of silicon from the (111) surface three bulk bonds have to be broken. Hence, the activation energy should be higher in comparison with the (100) etching process. In case of KOH, we have contradictory experimental data: H. Seidel with co-authors⁽⁶⁾ found (111) activation energy to be 0.1 eV higher than (100); that is in agreement with their model. M. Shikida⁽²³⁾ estimated (111) activation energy to be 0.12 eV lower than (100). The latter is difficult to explain: it is possible only if the (111) surface had many defects, which makes the removal of silicon atoms from the surface much easier.

The (111) plane activation energy of etching in TMAH is estimated in papers⁽²²⁻²⁴⁾ and

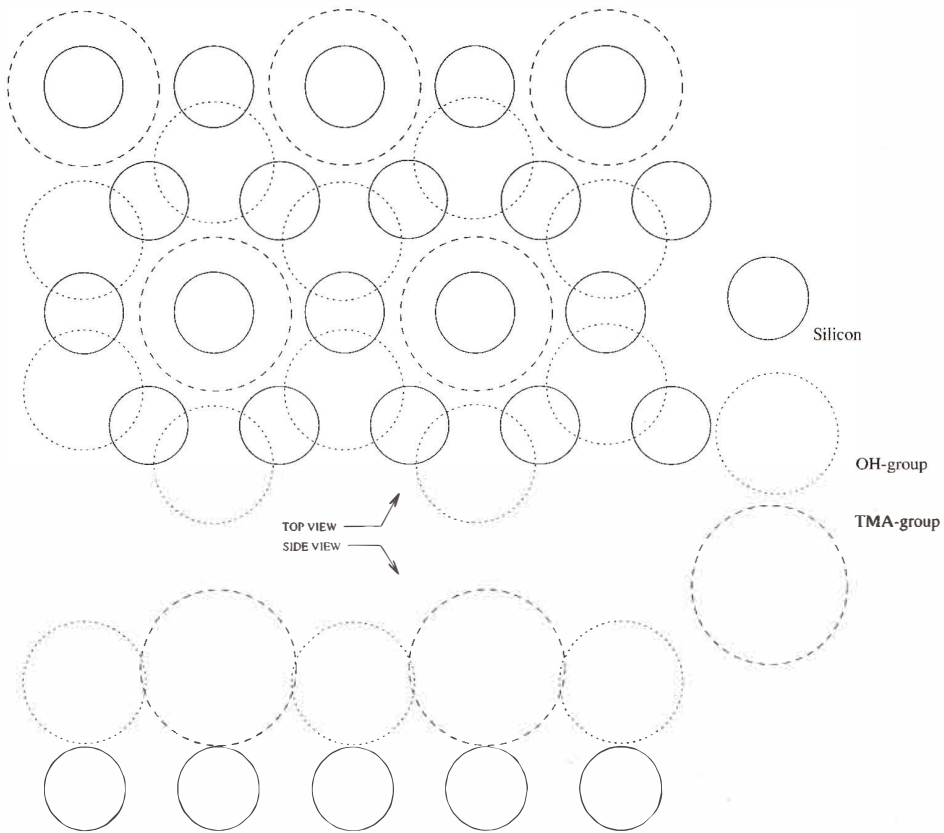


Fig. 4(▲). In this figure, the location of the TMA^+ groups is shown on top of the (111) plane silicon atoms, along with the locations of the OH groups.

this value is an issue as well. Our estimation (0.4 eV) coincides with lower activation energy obtained in refs. (22,24), and we consider these data to be more reliable. The lower activation energy in TMAH etching may be explained as follows.

Let us consider three neighboring surface silicon atoms connected in a chain. In order to remove those atoms, only six (not nine) bonds have to be broken, which means two bonds per atom, being equivalent to the (100) etching process. Correspondingly, the activation energy for this process of removal of a complex of three atoms has to be about 0.6 eV. The lower activation energy of about 0.4 eV, derived from experiments, means merely that less than two bonds per atom are being destroyed, and a complex, consisting of several (4 or more) silicon atoms connected to each other and a corresponding quantity TMA^+ and OH^- groups is being formed as an etching product. The removal of silicon atoms from the surface takes place in a zipper motion with various lengths of “zips”. An atom in a chain, that is going to be removed first, probably is in a kink position and has two

dangling bonds. This consideration explains why experimental data appear so scattered and indefinite: a number of different complexes with different quantities of silicon atoms is formed.

In order to confirm this model, the etch rate of the (110) silicon plane in NaOH and in TMAH was measured at different temperatures and corresponding activation energies were calculated (Fig. 2). In case of NaOH, we found $E_a = 0.61$ eV; that corresponds to a normal chemical reaction (removal of one silicon atom from the (110) surface in accordance with Seidel's model). But in case of TMAH, the activation energy is considerably smaller (0.42 eV), which may point to the formation of complexes mentioned above, or the same "zipper" mechanism of removal of silicon atoms from the surface.

Let us now look at the (110) silicon surface. Each silicon atom on the (110) plane has one "bulk" bond, one dangling bond and two bonds along the surface, so actually we have chains of the surface silicon atoms connected to each other and drawn out along the [110]

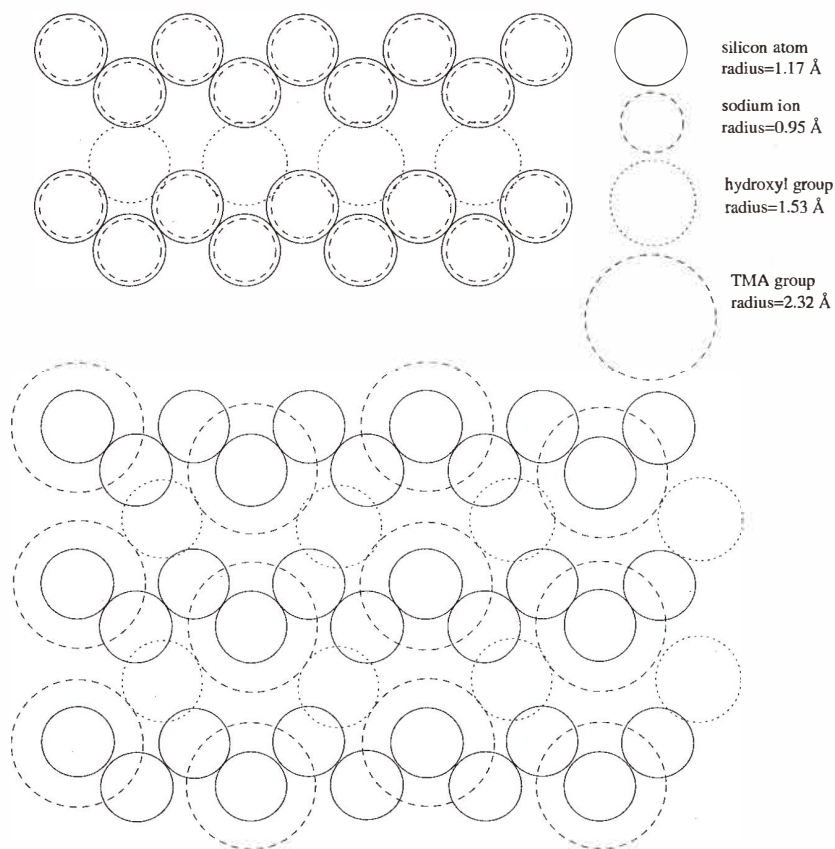


Fig. 5. Top view on the (110) silicon plane covered by Na⁺ ions (top) and by TMA⁺ group (bottom).

direction (Fig. 5).

There is sufficient space for OH-groups to interact with silicon both in case of NaOH and TMAH. The atoms may be removed as a chain so long as only one "bulk" bond (per atom) has to be destroyed. This means a lower activation energy, which we observed it in our experiments.

4. Conclusion

The etch rates of (100) and (110) silicon wafers in NaOH and TMAH have been measured as a function of temperature. The activation energies of 0.68 eV and 0.61 eV for NaOH etching for (100) and (110) planes have been calculated, which can respectively be interpreted as the "silicon (100) and (110) surface energy gap". The activation energy of etching of the (110) planes in TMAH is found to be lower, 0.42 eV (0.4 eV in ref. (22)) ; apparently because of the formation of complexes including several silicon atoms connected together.

At the same time, the {111}-plane etch rate is evaluated to be extremely low in NaOH: at lower temperatures, less than 50–60°C, we observed no underetching in the [110] direction in any slot with an arbitrary orientation on the (100) wafers, except in the [110] direction, which is attributed to the presence of defects. At higher temperatures the silicon dioxide mask etch rate starts to be non-negligible. The roughness of the surface etched by KOH was studied in ref. (26) and an influence of the mask junction was investigated in refs (27,28). We explain the roughness of the inclined surfaces of slots and their slopes as being due to the fact that there are always mask edge irregularities and defects, resulting in the formation of {111} planes where the etching process considerably slows down.

This is in sharp contrast to the situation in TMAH, where the {111} planes were etched at a higher etch rate so the smooth inclined surfaces of slots were observed.

References

- 1 D. F. Weirauch: *J. Applied Physics* **46** (1975) 1478.
- 2 D. L. Kendall, G. R. de Guel and A. Torres-Jacome: *Extended Abstracts* 82, *Electrochem. Soc.*, Abstract No. 132 (1982) p. 209.
- 3 O. J. Glembocki, E. D. Palik, G. R. de Guel and D. L. Kendall: *J. Electrochem. Soc.* **138** (1991) 1055.
- 4 H. Seidel: *Transducers'87, Rec. of the 4th Int. Conf. on Solid State Sensors and Actuators*, 1987, p. 120.
- 5 G. R. de Guel, D. L. Kendall and R. Galeazzi: *Extended Abstracts, Electrochem. Soc.*, Abstract No. 518, p. 758.
- 6 H. Seidel, L. Csepregi, A. Heuberger and H. Baumgartel: *J. Electrochem. Soc.* **137** (1990) 3612.
- 7 P. Allongue, V. Costa-Kieling and H. Gerischer: *J. Electrochem. Soc.* **140** (1993) 1018.
- 8 K. Sato, A. Koide and S. Tanaka, *JIEE Technical Meeting Micromachining and Micromechatronics*, 1989, Tokyo, IIC-89-30, p. 9.
- 9 A. Koide, K. Sato and S. Tanaka: *Proc. IEEE MEMS-91 (Nara, 1991-1)* p. 216.
- 10 C. H. Sequin: *Proceedings of Transducers '91*, p. 801.

- 11 K. Asaumi, Y. Iriye and K. Sato, Proc. of IEEE MEMS'97 (Nagoya 1997, Jan. 26-30) p. 412.
- 12 J. Fruehauf, K. Trautmann, J. Wittig and D. Zielke: J. Micromech. Microeng. **3** (1993) 113.
- 13 E. van Veenendaal, A. J. Nijdam, J. van Suchtelen, K. Sato, J. G. E. Gardeniers, W. J. P. van Enckevort and M. Elwenspoek: Sensors and Actuators A **84** (2000) 324.
- 14 A. Horn, F. Wittmann and G. Wachutka: Sensors and Materials **13** (2001) 315.
- 15 E. D. Palik, J. W. Faust Jr. and H. F. Gray: J. Electrochem. Soc. **129** (1982) 2051.
- 16 E. D. Palik, H. F. Gray and P.B.Klein: J. Electrochem. Soc. **130** (1983) 956.
- 17 O. J. Glembocki, R. E. Stahlbush and M. Tomkiewicz: J. Electrochem. Soc. **132** (1985) 145.
- 18 E. D. Palik, V. M. Bermudez and O. J. Glembocki; J. Electrochem. Soc. **132** (1985) 871.
- 19 L. M. Landsberger, M. Kahrizi, M. Paranjape and S. Naseh, Sensors and Materials **9** (1997) 417.
- 20 S. Naseh, L. M. Landsberger, M. Paranjape and M. Kahrizi: Canadian J. of Physics **74** Suppl. 1 (1996) S79.
- 21 A. Pandey, L. M. Landsberger, B. Nikpour, M. Paranjape and M. Kahrizi: J. of Vacuum Sci. & Technology A. Vacuum surfaces and Films **16** (1998) 868.
- 22 O. Tabata, R. Asahi, H. Funabashi, K. Shimaoka and S. Sugiyama: Sensors and Actuators A **34** (1992) 51.
- 23 M. Shikida, K. Sato, K. Tokoro and D. Uchikawa: Sensors and Actuators A **80** (2000) 179.
- 24 O. Tabata: Sensors and Materials **13** (2001) 271.
- 25 P. Allongue, V. Kosta-Kieling and H. Gerischer: J. Electrochem. Soc. **140** (1993) 1009.
- 26 K. Sato, M. Shikida, T. Yamashiro, M. Tsunekawa and S. Ito: Sensors and Actuators A **73** (1999) 122.
- 27 A. J. Nijdam, J. W. Berenschot, J. van Suchtelen, J. G. E. Gardeniers and M. Elwenspoek: J. Micromech. Microeng. **9** (1999) 135.
- 28 E. van Veenendaal, H. M. Cuppen, W. J. P. van Enckevort, J. van Suchtelen, A. J. Nijdam, M. Elwenspoek and E. Vlieg: J. Micromech. Microeng. **11** (2001) 409.

About the Authors

Vladimir F. Kleptsyn graduated from Moscow Steel and Alloys Institute, Department of Material Science of Semiconductors in 1975 (M.S.) and from Moscow University of Fine Chemical Technology, Department of Technology of Semiconductor Materials in 1981. He received his Ph.D. Degree in 1983. From 1982 until 1994 he was a team and projects leader at the Research Institute of Materials for Electronic Technics (Russia). From 1994 until 1998, he was a research manager in Antrel Ltd, Moscow. Since April 1999, he has been employed as an Engineer/Researcher at Boston University, Electrical and Computer Engineering Department. His current research interests include silicon process, etching of silicon, and MEMS.

Johannes G. Smits obtained the degree of Candidate in Physics (1966) and the degree of Doctorandus in Physics (1970) from the University of Leyden. Subsequently he studied electronics at Twente University until 1973. Then he joined the Electronics Materials Research Group and did his Ph.D. research on piezoelectric ceramics. In 1979 he joined the Sensor Group of Professor Angell at Stanford University, where he worked on the design of an integrated pressure sensor, and in the E.Ginzton Lab he worked with Professor Khuri-Yakub on the improvement of the sputtering process of piezoelectric ZnO on silicon.

Following this he returned to the Netherlands where, along with his colleagues at Twente University, he initiated and built the Sensors and Actuators Laboratory, of which he was the chairman of the Board of Supervisors. He invented resonant integrated pressure and force sensors and laser beam deflectors as well as an integrated micropump for the delivery of insulin to diabetes patients.

In 1985 he joined the faculty of Boston University as an Associate Professor, where he continues his work on micromechanical silicon devices. He works on integrated accelerometers, tactile sensors, strain gauges and microrobots. He is currently involved with the fabrication of integrated bimorph laser beam deflectors, integrated DNA sequencing sensors, micropumps for the analysis of the Mars atmosphere, and various other devices.

He is a Fellow of the IEEE, an Associate Editor for microelectromechanical systems and piezoelectric thin film devices of the IEEE Transactions on Ultrasonics, Ferroelectrics and Frequency Control, and a member of the Technical Program Committee of the IEEE Ultrasonics Symposium.